Genes, Brain and Behavior
Official publication of the International Behavioural and Neural Genetics Society

Genes, Brain and Behavior (2009) **8:** 181–192

Behavioral characterization of mice lacking the neurite outgrowth inhibitor Nogo-A

R. Willi[†,‡,1]*, E. M. Aloy[†,‡,1], B. K. Yee[§], J. Feldon[§] and M. E. Schwab[†,‡]

[†]Brain Research Institute, University of Zurich, and [‡]Department of Biology, ETH Zurich, Zurich, and [§]Laboratory of Behavioral Neurobiology, Department of Biology, ETH Zurich, Schwerzenbach, Switzerland

**Corresponding author: R. Willi, Brain Research Institute, University of Zurich, and Department of Biology, ETH Zurich, Winterthurerstrasse 190, 8057 Zurich, Switzerland. E-mail: rwilli@hifo.uzh.ch*

The membrane protein Nogo-A inhibits neurite outgrowth and regeneration in the injured central nervous system, primarily because of its expression in oligodendrocytes. Hence, deletion of Nogo-A enhances regeneration following spinal cord injury. Yet, the effects of Nogo-A deletion on general behavior and cognition have not been explored. The possibility of potential novel functions of Nogo-A beyond growth inhibition is strongly suggested by the presence of subpopulations of neurons also expressing Nogo-A – not only during development but also in adulthood. We evaluated here *Nogo-A*$^{-/-}$ mice in a series of general basic behavioral assays as well as functional analyses related to brain regions with notable expression levels of Nogo-A. The SHIRPA protocol did not show any major basic behavioral changes in *Nogo-A*$^{-/-}$ mice. Anxiety-related behavior, pain sensitivity, startle reactivity, spatial learning, and associative learning also appeared indistinguishable between *Nogo-A*$^{-/-}$ and control *Nogo-A*$^{+/+}$ mice. However, motor co-ordination and balance were enhanced in *Nogo-A*$^{-/-}$ mice. Spontaneous locomotor activity was also elevated in *Nogo-A*$^{-/-}$ mice, but this was specifically observed in the dark (active) phase of the circadian cycle. Enhanced locomotor reaction to systemic amphetamine in *Nogo-A*$^{-/-}$ mice further pointed to an altered dopaminergic tone in these mice. The present study is the first behavioral characterization of mice lacking Nogo-A and provides significant insights into the potential behavioral relevance of Nogo-A in the modulation of dopaminergic and motor functions.

Keywords: Activity, dopamine, growth inhibition, knockout mice, learning, memory, motor behavior, Nogo-A

Received 10 July 2008, revised 24 October 2008, accepted for publication 24 October 2008

[1]These authors contributed equally to this work.

Regeneration of injured fibers in the adult central nervous system (CNS) is limited partly by neurite growth inhibitory molecules present particularly in myelin (Caroni & Schwab 1988a,b; Filbin 2003; Schwab 2002, 2004); and Nogo-A is one such major potent neurite growth inhibitor (Chen *et al.* 2000; GrandPre *et al.* 2000; Prinjha *et al.* 2000; Spillmann *et al.* 1998). Nogo-A neutralizing antibodies can enhance regeneration and functional recovery after CNS damage (Brosamle *et al.* 2000; Gonzenbach & Schwab 2008; Liebscher *et al.* 2005; Merkler *et al.* 2001; Schnell & Schwab 1990). Similarly, Nogo-A knockout mice also exhibit enhanced regenerative abilities following spinal cord injury (Dimou *et al.* 2006; Kim *et al.* 2003; Simonen *et al.* 2003). Nogo-A therefore represents a major target for control of growth/regrowth in the CNS, but its potential functional relevance beyond that has not been well characterized. Moreover, it is still not known whether the altered growth responses observed after Nogo-A deletion would be associated with changes in neuronal networks or circuits that in turn would lead to altered behavior. The answer to this question is of utmost relevance to the ongoing clinical trials with anti-Nogo-A antibody treatment in spinal cord injured patients.

It is now known that Nogo-A is not exclusively expressed in oligodendrocytes as previously thought. Messenger RNA and protein localization studies have shown that also subsets of neurons in cerebellum, hippocampus, retina, and dorsal root ganglia express Nogo-A (Huber *et al.* 2002; Hunt *et al.* 2003; Josephson *et al.* 2001; Wang *et al.* 2002). Notably, neuronal expression of Nogo-A is especially high during development but is downregulated in most adult neuronal populations, except in selected regions of high plasticity, for example hippocampus (Huber *et al.* 2002; Meier *et al.* 2003). The developmental and regional expression pattern of Nogo-A strongly suggests that it may assume functions beyond neurite growth inhibition, for example in neurodevelopment and neural plasticity, although these possibilities have not been comprehensively evaluated. The present study represents the first attempt in this direction by characterizing the impact of constitutive Nogo-A deletion on general behavioral brain functions in adult animals, paving the way for future studies with more specific molecular manipulations and refined behavioral analysis.

In this study, we first employed the SHIRPA protocol for a qualitative assessment of abnormal behavioral traits in Nogo-A knockout mice. Cerebellum-dependent motor coordination and balance were evaluated next (Lalonde & Strazielle 2007; Llinas & Welsh 1993) because specific cerebellar neurons are known to strongly express Nogo-A (Aloy *et al.* 2007; Huber *et al.* 2002; Hunt *et al.* 2003). As Nogo-A is also expressed in the perinatal retinal ganglion cell layer and the hypothalamus (Funahashi *et al.* 2008; Huber

doi: 10.1111/j.1601-183X.2008.00460.x

et al. 2002; Hunt *et al.* 2003; Liu *et al.* 2002; V. Pernet, personal communication), we also investigated here the circadian rhythm of general locomotor activity, which depends on photoreception via retinal ganglion cells (Cermakian & Sassone-Corsi 2000, 2002) and their anatomical links to circadian centers located in various hypothalamic nuclei (Guilding & Piggins 2007). Because the hippocampus is another brain area with high Nogo-A levels (Huber *et al.* 2002; Hunt *et al.* 2003; Meier *et al.* 2003), hippocampal-sensitive behavior, such as anxiety, associative learning and spatial learning (Bannerman *et al.* 2004; Davidson & Jarrard 2004), was also examined here.

Materials and methods

Animals

The subjects were all adult male mice with an F_1 C57BL/6J × 129X1/SvJ hybrid background, containing one copy of each gene from each of the two constituent pure inbred strains, as recommended by the Banbury Conference on Genetic Background in Mice (1997).

Nogo-A$^{+/-}$ × *Nogo-A*$^{+/-}$ breeding (≥10 generations) independently in the C57BL/6J and 129X1/SvJ background allowed the generation of *Nogo-A*$^{-/-}$, *Nogo-A*$^{+/-}$ and *Nogo-A*$^{+/+}$ littermates in each background strain in parallel. *Nogo-A*$^{-/-}$ and *Nogo-A*$^{+/+}$ littermates (from both strains) were paired as described below to produce the experimental subjects used in the present study. Nogo-A knockout mice were F_1 hybrid mice generated by interstrain crossing of *Nogo-A*$^{-/-}$ mice. In parallel, age-matched control wild-type (*Nogo-A*$^{+/+}$) F_1 hybrid mice were obtained from interstrain crossing of *Nogo-A*$^{+/+}$ mice. In each experiment, the subjects were always derived from multiple litters. Full details of the initial generation of the *Nogo-A*$^{-/-}$ mouse line have been reported before (Dimou *et al.* 2006; Simonen *et al.* 2003). Standard polymerase chain reaction procedures were used to verify the animals' genotype using genomic DNA isolated from tail tips as previously described (Simonen *et al.* 2003).

The animals were housed on a reversed 12/12-h light/dark cycle (lights on at 2000 h) under temperature-controlled (21°C) and humidity-controlled (55%) conditions. Littermates were caged in groups of four to eight and maintained with *ad libitum* food and water. Behavioral testing was carried out when the mice were 2–4 months old and took place during the dark phase of the light/dark cycle (except for the 24-h monitoring of home cage activity experiment). All animals were experimentally naive except in the Plantar Heater test used to assess pain sensitivity and the test for amphetamine (AMPH)-induced locomotor activity. The exact number of mice used in each experiment is clearly specified in each respective results section. All procedures described in the present study had been approved by the Cantonal Veterinary Office in Zurich and are in agreement with the Principles of Laboratory Animal Care (National Institutes of Health Publication no. 86–23, revised 1985).

SHIRPA protocol – primary screen

The SHIRPA primary screen is a standardized battery of tests designed to provide a behavioral and functional profile of mice by observational assessment. The protocol was carried out as described in full details elsewhere (Rogers *et al.* 1997; also see www.mgu.har.mrc.ac.uk/mutabase/shirpa_1.html).

Briefly, each mouse was first placed into a viewing jar (perspex cylinder, 15 cm in diameter), which was located on top of a grid. Body position and activity, as well as pathological signs such as respiratory difficulties and body tremor, were evaluated for 5 min. The number of defecations was also counted. The animal was then transferred to an arena (transparent perspex box, 55 × 33 × 18 cm) containing 15 squares on the floor (11 × 11 cm). Transfer arousal and locomotor activity (as the number of square crossings over 30 s) were then recorded. The following behaviors were measured next: eye opening, piloerection, the startle response to a 90 dB sound from a clickbox, gait, pelvic and tail elevation. The mouse was then stroked from above for evaluating touch escape, and the struggle response to sequential handling was subsequently examined. Lowering the animal by the tail toward a wire grid allowed assessment of trunk curl, limb grasping and visual placing responses. Grip strength exerted on the wire was tested by gently pulling the mouse by the tail. While the mouse was gently restrained, body tone, toe pinch, pinna and corneal reflexes were checked. The animals' forepaws were then placed onto a horizontal wire bar, and its ability to lift the hindlimbs and remain on the wire (wire maneuver) was evaluated. Thereafter, the mouse was held in a restraint supine position for assessment of skin color, heart rate, abdominal and hindlimb tone, lacrimation, salivation as well as a biting response provoked by a plastic probe. Next, the righting reflex was tested by observing the animals' landing position after performing a somersault. In the contact righting reflex test, the mouse was placed inside a small plastic tube and then rotated to check whether it is able to return to the original body position. The negative geotaxis test consisted in placing the animals face down on a vertically oriented grid, and noting the ability to turn and climb toward the top. The test battery was then completed with general estimations of fear, irritability, aggression, vocalization, body weight as well as unusual neurological signs, such as paw clasping. Seven behavioral characteristics that are representative of the behavioral categories assessed in the SHIRPA primary screen are displayed in the *Results* part in detail.

Plantar heater test

The level of nociception for hindpaws was evaluated by performing the standardized plantar heater test (Ugo Basile Biological Research Apparatus, Comerio, Italy) with an infrared source producing a calibrated heating beam (diameter 1 mm) as described before (Liebscher *et al.* 2005). The mice tested in this experiment had already undergone the SHIRPA primary screen. After one initial measurement, the latency for paw withdrawal was determined in four successive trials per hindpaw with an intertrial interval (ITI) of 5 min, and expressed as mean latency over all test trials.

Acoustic startle response

Acoustic startle reactivity was assessed by using a set of four acoustic startle chambers (SR-LAB; San Diego Instruments, San Diego, CA, USA) as previously described (Pietropaolo *et al.* 2008a, b). Vibrations of the Plexiglas enclosure (which housed the animal during test) caused by the animal's whole-body startle response were recorded. A series of discrete trials comprising various acoustic white noise stimuli was presented in a trial-discrete manner against a constant background noise level of 65 dB_A. Stimuli of various intensities were used: 69, 73, 77, 81, 85, 90, 95, 100, 110 and 120 dB_A at either 20 ms or 40 ms in duration.

A session began with the animals being placed into the Plexiglas enclosure. The first trial began after a 2-min acclimatization period. The first six trials were performed with the highest intensity acoustic stimulus (120 dB_A: at 20 ms duration in three trials and 40 ms in the other three) to habituate and stabilize the animals' startle response. Subsequently, there were five blocks of discrete trials. Each block consisted of 20 trials, one for each stimulus intensity and stimulus duration. All trials were presented in a pseudorandom order, and the interval between successive trials was variable, with a mean of 15 s.

Accelerating rotarod

This test measures motor co-ordination on a rotating rod (Crawley 2000; Crawley *et al.* 1997). The device consisted of a rotating drum divided into five separate lanes by opaque disks (Ugo Basile Biological Research Apparatus). Each lane had its own digital timer and display. The experiment was conducted as previously described (Aloy *et al.* 2007). Mice were placed on the appropriate lanes and the timers were started. The rotation rate of the drum was linearly increased from 4 to

40 r.p.m. over a period of 5 min. A trial ended when the animal fell off the rotating drum and thereby activating the landing pad that stopped automatically the timer, or when a maximum of 5 min had elapsed. The latency to fall was recorded to index performance. Each mouse was given four trials per day with an ITI of 1 h over three consecutive days.

Spontaneous activity and circadian rhythm

Circadian locomotion was assessed in 16 chambers made of Plexiglas, each located within a sound-attenuating wooden cabinet. The mice were kept individually to each chamber undisturbed throughout the duration of the experiment for 14 days. Each chamber measured 25 × 40 × 40 cm. Food was accessible from the food hopper mounted on one side wall through a metal grid; water was provided by a drinking bottle with its drinking sprout protruding into the same side wall. The floor tray was filled with rodent sand (Acapulco Badesand; Qualipet AG, Dietlikon, Switzerland) to provide a light background to allow effective detection of the subjects. Illumination within each chamber was provided by a 4-W light, which was controlled by a timer programmed to be switched on daily from 2000 h to 0800 h. A ventilation fan was mounted on the back wall of each cabinet that also provided a stable level of background noise. A digital camera was positioned 49 cm above the area of interest in each chamber to allow continuous assessment of locomotor activity with a software developed in-house (P. Schmid, Laboratory of Behavioral Neurobiology, ETH Zurich; Russig *et al.* 2003). Briefly, successive 8-bit gray-scale images at 1-s apart were compared and the number of pixels differing between the two images were quantified and expressed as percentage pixel change relative to the total pixels in each frame (Richmond *et al.* 1998). To index circadian locomotor activity rhythm, the activity measure (percent second-by-second pixels changes) was averaged to provide an hourly score.

Locomotor reaction to systemic AMPH

The test for AMPH-induced locomotor activity was conducted in the activity chambers described above, and the mice used here had already undergone the spontaneous activity experiment. On the first day of the experiment, the animals were removed from the apparatus, injected with vehicle (isotonic 0.9% NaCl, intraperitoneally, injection volume of 5 ml/kg) solution and immediately placed back into the chambers. Locomotor activity was then measured for 3 h as described before. Forty-eight hours after the vehicle injection, they were again removed from the apparatus and then administered with D-amphetamine sulfate (2.5 mg/kg, intraperitoneally, injection volume of 5 ml/kg). They were then immediately returned to the same chamber again, and the locomotor response to the acute drug challenge was monitored for another period of 3 h. The activity data from the two phases of the experiment were quantified across successive 10-min bins.

Elevated plus maze

This test allows the assessment of anxiety-like behavior in rodents (Handley & Mithani 1984; Lister 1987; Pellow *et al.* 1985). An opaque and a transparent Plexiglas plus maze were used in the current study, as variation in the transparency of the closed arms has been suggested to ameliorate interpretation of elevated plus maze behavior particularly in transgenic mice (Hagenbuch *et al.* 2006). Each maze consisted of two open (30 × 5 cm) and two enclosed arms (30 × 5 × 15 cm). The arms radiated from a central platform (5 × 5 cm), and the entire apparatus was raised to a height of 70 cm above floor level. Testing was carried out under dim lighting conditions (30 lx in the open arms of the mazes). The test session started when the animal was placed on the central platform facing an open arm. The mouse was then allowed to freely explore the maze for 5 min. A digital camera was mounted above the maze. Images were captured at a rate of 5 Hz and transmitted to a PC running the Ethovision tracking system (Noldus Technology, Wageningen, The Netherlands). The following measures were computed: Percent open arm entries [open arm entries/(open + closed arm entries) × 100%], percent time spent in the open arms [time in open arms/(time in open + closed arms) × 100%], and total distance traveled (in cm).

Conditioned freezing

Next, we investigated the acquisition, retention and extinction of a conditioned response acquired through Pavlovian fear conditioning (Maren 2001). The experiment was performed using two sets (identified here as context A and context B) of four chambers as fully described by Meyer *et al.* (2005). Conditioning and the subsequent test of context freezing were conducted in context A, whereas tests of conditioned freezing to the tone conditioned stimulus (CS) were conducted in context B.

Briefly, context A consisted of four metal operant boxes (30 × 25 × 29 cm; model E10-10; Coulbourn Instruments, Allentown, PA, USA), each installed in a ventilated and sound-insulated Coulbourn Instruments chest. The animal was confined to a rectangular enclosure (17.5 × 13 cm) in the middle of the operant box. The grid floor was made of stainless steel rods (4 mm in diameter) spaced at 10 mm intervals center to center, through which scrambled electric shocks [unconditioned stimulus (US); 0.25 mA] could be delivered (model E13-14; Coulbourn Instruments). Constant illumination was provided by a 2.8-W incandescent house light in each chamber. Context B comprised four semicircular (19 cm in diameter) Plexiglas enclosures resting on a smooth plastic floor. Each chamber was installed in a ventilated, sound-insulated, wooden cabinet and with illumination similar to that described for context A.

All chambers were equipped with a sonalert (model SC628; Mallory, Indianapolis, IN, USA) for the delivery of an 86 dB_A tone serving as the CS. In addition, a digital camera was mounted 30 cm directly above the area of interest in each chamber, and images were captured at a rate of 1 Hz. Freezing behavior was evaluated by comparing successive frames as described before (Richmond *et al.* 1998).

The test procedures consisted of three phases: conditioning (context A), context test (context A) and tone tests (context B). Conditioning comprised three successive trials of CS–US pairings. Each trial began with the 30-s tone stimulus followed immediately by the delivery of a 1-s foot shock. Each trial was preceded and followed by a 180-s interval (ITI). The context test took place 24 h later, when the subjects were returned to the same chambers for a period of 480 s in the absence of any discrete stimulus. The tone test, assessing the conditioned response to the tone CS, was conducted another 24 h later. Following a 180-s acclimatization period, the tone was turned on for 480 s. The tone test was repeated again 24 and 48 h later, thus allowing the evaluation of extinction of the conditioned response between-days.

For the conditioning session, the percentage of time spent freezing during the 30-s tone presentations and across successive 180-s ITIs was calculated. The percentage time freezing was expressed in 1-min bins for the context and tone test sessions.

Two-way active avoidance learning

This task captures both elements of classical and instrumental conditioning, in which the animals learned to perform a specific operant act in response to a tone stimulus to avoid the delivery of an aversive foot shock (i.e. negative reinforcement). The apparatus consisted of four identical two-way shuttle boxes (model H10–11M-SC; Coulbourn Instruments) as fully described before (Meyer *et al.* 2008). Electric shocks (0.3 mA) could be delivered through the grid floor that was connected to a constant current shock generator (model H10–1M-XX-SF; Coulbourn Instruments). The CS was an 86-dB_A tone generated by a tone module (model E12-02; Coulbourn Instruments). Shuttle responses were detected by a series of photocells (H20–95X; Coulbourn Instruments) mounted on the side of both shuttle compartments.

Animals were placed in the shuttle chambers and received a total of 100 conditioned avoidance trials presented according to a sequence

of random ITIs of 40 ± 15 s. The first trial started after an initial interval of an average of 40 s. A trial began with the onset of the tone CS. If the animal shuttled within 5 s of CS onset, the CS was terminated and the animal avoided the electric shock on that trial. Avoidance failure led immediately to an electric foot shock presented in coincidence to the CS. This lasted for a maximum of 2 s but could be terminated earlier by a shuttle response during this period (i.e. an escape response). To index conditioned avoidance learning, the mean number of avoidance shuttles performed across successive 20-trial blocks was calculated. To index general locomotor activity, the number of spontaneous shuttles performed during ITIs was also recorded.

Spatial learning in the Morris water maze

Spatial learning was assessed using the Morris water maze. The water maze consisted of a white circular tank made of fiberglass (diameter 102 cm, height 36 cm) and was positioned in the middle of a well-lit testing room enriched with distal visual cues. The water maze was daily filled with fresh tap water to a depth of 19 cm, and the temperature was maintained at 24 ± 1°C. A transparent solid Plexiglas cylinder (diameter 12 cm, height 18.5 cm) was used as an escape platform. Its top was submerged 0.5 cm below the water surface, remaining invisible to the animals. It could be made visible by mounting a white circular disk (diameter 12 cm), 10 cm above the platform. A digital camera was installed above the maze. Images were captured at a rate of 5 Hz and transmitted to a PC running the Ethovision tracking system (Noldus Technology).

On the first day, the animals were pretrained in the water maze using the visible platform (positioned in the center of the maze) for two consecutive trials. This served to familiarize the animals with the water maze. To begin a trial, an animal was gently placed into the water against the maze wall at one of the four cardinal positions (N, E, S or W). An animal was allowed a maximum of 60 s to locate the escape platform. It was guided to the platform by the experimenter if it failed to locate the platform within 60 s. The mouse was allowed to spend 15 s (ITI) on the platform before commencement of the next trial. All animals acquired the swimming response and were able to climb onto the escape platform.

To assess reference memory, the animals were then trained to locate the hidden platform over the next 5 days (days 2–6). The platform location was positioned at a fixed location in the middle of one of the four quadrants (NE, SE, SW or NW) and the allocation of the target quadrant was counterbalanced across subjects. The animals were trained for four trials per day with an ITI of 15 s and the starting position randomly varied from trial to trial among the four possible positions (N, E, S and W). The sequence of starting positions across trials also varied from day to day. The escape latency, path length and average swim speed were recorded in every trial. On day 7, a probe trial was performed in which the platform was removed from the maze and each animal's search pattern was evaluated for 60 s. Each animal was released from a location opposite to its target quadrant. The percentage time spent in each quadrant and the number of crossings over the former platform location (annulus crossings) was calculated to index search accuracy.

To assess reversal learning, animals were trained over the next 3 days (days 8–10) as described for the reference memory task except that the location of the platform was moved to the middle of the opposite quadrant. On the next day (day 11), another probe test was performed as described above.

Statistics

All behavioral data (except SHIRPA primary screen scores) were subjected to parametric analysis of variance (ANOVA) of the appropriate design, followed by supplementary restricted ANOVAs to assist data interpretation whenever adequate. *Post hoc* pairwise comparisons were performed using Fisher's least significant difference (LSD) test (based on the relevant pooled error variance from the ANOVA table) with appropriate Bonferroni correction. Data from startle reactivity were logarithmically (based *e*) transformed before analysis to better conform to the assumptions of parametric ANOVA. Scores obtained in the SHIRPA primary screen were analyzed using the Mann–Whitney *U*-test. All statistical analyses were conducted using the statistical software SPSS for Windows (release 14.0; Chicago, IL, USA).

Results

Behavioral performance in the SHIRPA primary screen is not affected in mice lacking Nogo-A

We assessed a general behavioral observation profile using the standardized SHIRPA primary screen. No genotype effect was detected for any of the scored measures ($n = 12$/group). Figure 1 depicts seven behavioral characteristics that are representative of the behavioral categories addressed: grip strength ($U = 72.0$, $P = 1.000$), corneal reflex ($U = 66.0$, $P = 0.755$), toe pinch ($U = 58.0$, $P = 0.443$), fear ($U = 66.0$, $P = 0.755$), irritability ($U = 60.0$, $P = 0.514$), vocalization ($U = 54.0$, $P = 0.319$) and locomotor activity ($U = 53.5$, $P = 0.291$). Together, these data do not suggest the presence of any gross neurological or physical abnormalities in the *Nogo-A*$^{-/-}$ mice.

Pain sensitivity is not affected in mice lacking Nogo-A

The plantar heater test was used to test pain sensitivity. *Nogo-A*$^{-/-}$ and *Nogo-A*$^{+/+}$ mice ($n = 12$/group) displayed comparable latency in paw withdrawal (mean withdrawal latency in seconds ± SEM = 1.86 ± 0.15 vs. 1.65 ± 0.17, respectively). The main effect of genotype was far from statistical significance ($F < 1$). Hence, there was no evidence

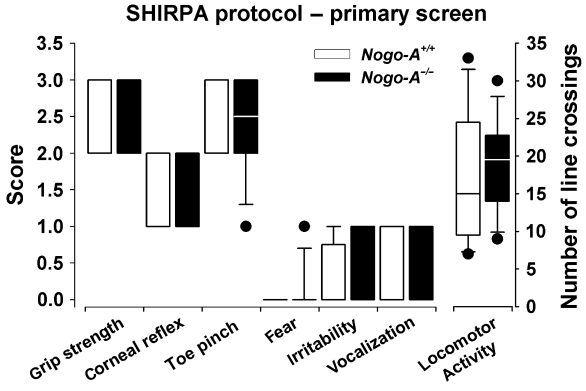

Figure 1: No effect of Nogo-A deletion on behavioral performance in the SHIRPA primary screen. Scores for seven behavioral features that are representative of all behavioral categories tested are shown. Grip strength was scored from 0 (absence of grip) to 3 (strong grip). Paw withdrawal response to toe pinch was scored from 0 (no withdrawal) to 3 (fast withdrawal). Corneal reflex was scored from 0 (no eyeblink reflex) to 2 (multiple eyeblinks). Fear, irritability and vocalization were scored 0 (absence) or 1 (present). Locomotor activity was scored as number of squares entered by all four feet within 30 seconds. Values are expressed as box plots showing median, 25th and 75th percentiles, and outliers; $n = 12$/group.

to suggest that the two groups differed in the perception or reaction to painful stimulation.

Acoustic startle reactivity is not affected in mice lacking Nogo-A

Next, reaction to external stimulation was evaluated by assessment of the whole-body startle reflex. Acoustic stimuli in the form of white noise across a wide range of intensities were used. As shown in Fig. 2, the magnitude of the startle reaction increased monotonically with increasing stimulus intensity; and the two groups of mice ($n = 7$/group) showed highly similar response magnitudes across the range of stimuli. A 2 × 2 × 10 (genotype × stimulus duration × stimulus intensity) split-plot ANOVA of (ln-transformed) reactivity showed a main effect of stimulus intensity ($F_{9,108} = 24.54$, $P < 0.001$). Neither the main effect of genotype ($F < 1$) nor its interaction with stimulus intensity ($F < 1$) was significant. The startle reaction was not dependent on stimulus duration (Fs < 1). Hence, there was no evidence for any difference in startle reactivity in mice lacking Nogo-A.

Improved motor co-ordination in mice lacking Nogo-A

Motor co-ordination and balance was assessed using the accelerating rotarod test (Fig. 3). A 2 × 3 × 4 (genotype × days × trials) split-plot ANOVA of latency to fall pointed to a general improvement in motor performance within as well as between days ($n = 15$/group; days: $F_{2,56} = 37.96$, $P < 0.001$; trials: $F_{3,84} = 6.80$, $P < 0.001$; days × trials: $F_{6,168} = 7.13$, $P < 0.001$). However, *Nogo-A*$^{-/-}$ mice displayed a significant improvement in motor co-ordination compared with *Nogo-A*$^{+/+}$ mice (genotype: $F_{1,28} = 8.19$; $P < 0.01$). This effect appeared to be stable over days and trials, as suggested by the lack of any interaction with the factor genotype (genotype × days: $F_{2,56} = 1.74$, $P = 0.185$; genotype × trials: $F_{3,84} = 1.25$, $P = 0.298$).

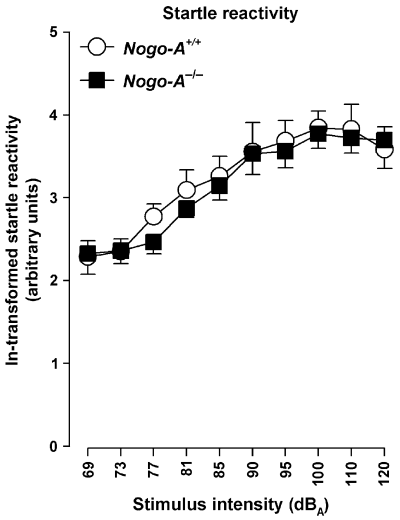

Figure 2: Normal acoustic startle reactivity in *Nogo-A*$^{-/-}$ mice. The (ln-transformed) intensity of startle reaction, expressed as a function of stimulus intensity and collapsed across the two-stimulus durations of 20 and 40 ms. Values are expressed as mean ± SEM; $n = 7$/group.

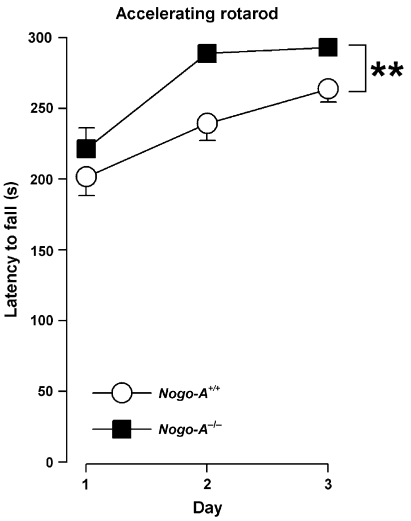

Figure 3: Increased motor co-ordination performance on the accelerating rotarod in *Nogo-A*$^{-/-}$ mice. Latency to fall in the accelerating rotarod task. *Nogo-A*$^{-/-}$ mice showed significantly enhanced motor co-ordination compared with wild-type mice. Values are expressed as mean ± SEM; $n = 15$/group. Asterisks (**$P < 0.01$) denote the significant difference between genotypes across the 3 days of testing.

Increased locomotor activity in mice lacking Nogo-A specific to the dark phase of the daily light–dark cycle

Locomotor activity was monitored continuously over 14 days under single-cage conditions, allowing the assessment of circadian rhythm of locomotor activity under a standard 12/12-h light/dark cycle ($n = 8$/group). As shown in Fig. 4a, activity exhibited a characteristic variation across the 24-h period. There was a clear reduction in the activity level over the course of the light phase, when *Nogo-A*$^{-/-}$ and *Nogo-A*$^{+/+}$ mice were largely comparable. This was followed by a more sustained elevation of activity in the dark phase, and *Nogo-A*$^{-/-}$ mice were consistently more active than *Nogo-A*$^{+/+}$ controls throughout this period of darkness. Thus, absence of Nogo-A was associated with increased spontaneous locomotor activity preferentially in the dark phase (Fig. 4b), which is the active phase for the murine species. These interpretations of the data were confirmed by a 2 × 14 × 2 × 12 (genotype × days × phases × hours) split-plot ANOVA of hourly activity data across the 14-day test period, which yielded a significant effect of phases ($F_{1,14} = 54.71$, $P < 0.001$), and of its interaction with genotype ($F_{1,14} = 6.55$, $P < 0.05$). The latter was indicative of the phase-specific hyperactivity effect seen in *Nogo-A*$^{-/-}$ mice, which was accompanied by a main effect of genotype just failing to attain statistical significance ($F_{1,14} = 4.13$, $P = 0.06$).

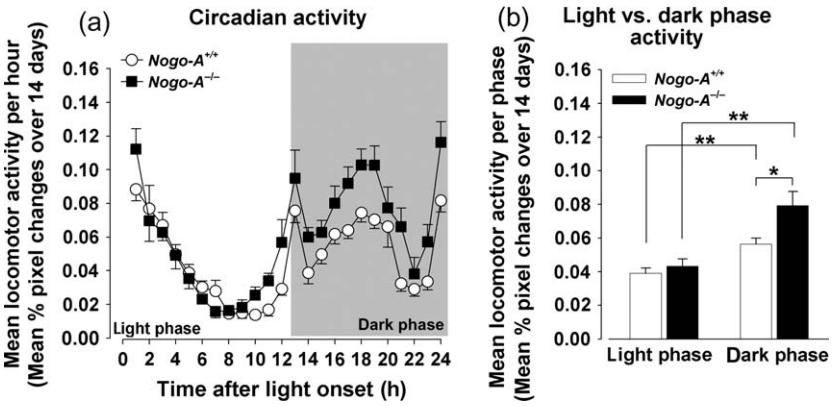

Figure 4: Increased locomotor activity during the dark phase in *Nogo-A*$^{-/-}$ mice. (a) Circadian activity across 14 days under a 12/12-h light/dark cycle, and (b) mean locomotor activity during the light vs. dark phase of the cycle. Both groups displayed a rhythmic circadian locomotion pattern (a). However, *Nogo-A*$^{-/-}$ mice showed higher activity during the dark phase of the cycle compared with *Nogo-A*$^{+/+}$ mice (a, b). Values are expressed as mean ± SEM; $n = 8$/group; $^{*}P < 0.05$, $^{**}P < 0.01$.

Supplementary analyses restricted to either phase showed that while the genotype effect was significant in the dark phase ($F_{1,14} = 5.23$, $P < 0.05$), it was far from being significant in the light phase ($F_{1,14} = 1.02$, $P = 0.329$). Finally, there was no indication that this effect of Nogo-A deletion varied significantly across days: neither the genotype × days interaction ($F < 1$) nor the genotype × days × phases interaction ($F_{13,182} = 1.21$, $P = 0.277$) approached statistical significance.

Increased sensitivity to systemic AMPH in mice lacking Nogo-A

Next, the locomotor response to AMPH was evaluated (Fig. 5). There was no significant difference between the groups after saline injection, as shown by a 2 × 18 (genotype × 10-min bins) split-plot ANOVA of locomotor activity (genotype: $F < 1$; genotype × 10-min bins: $F < 1$; Fig. 5a). Following injection of systemic AMPH, the locomotor activity of all animals clearly increased, but this effect was notably more pronounced in the *Nogo-A*$^{-/-}$ mice (Fig. 5b). This impression was confirmed by a 2 × 18 (genotype × 10-min bins) split-plot ANOVA, which yielded a significant effect of 10-min bins ($F_{17,238} = 23.17$, $P < 0.001$) and of its interaction with genotype ($F_{17,238} = 1.80$, $P < 0.05$; genotype: $F_{1,14} = 2.58$, $P = 0.130$).

Anxiety-like behavior is not affected in mice lacking Nogo-A

Here, we employed two designs of the elevated plus maze test of anxiety to assess whether Nogo-A deletion would be associated with either anxiogenesis or anxiolysis. In both test designs, no differences in anxiety-related behavior were detected between groups ($n = 12$/group). Analysis of either percent open arm entries (Fig. 6a) or percent time spent in open arms (Fig. 6b) failed to yield any genotype effect (Fs < 1).

As expected (Hagenbuch *et al.* 2006), the transparent maze promoted open arm exploration compared with the opaque one (percent open arm entries: $F_{1,44} = 60.24$, $P < 0.001$; percent time spent in open arms: $F_{1,44} = 25.85$, $P < 0.001$), and this effect was independent of genotype (genotype × maze interactions: percent open arm entries: $F_{1,44} = 1.61$, $P = 0.211$; time spent in open arms: $F < 1$; Fig. 6a,b). Total distance traveled (as an activity measure) in the maze did not differ between groups (genotype: $F_{1,44} = 2.71$, $P = 0.107$; data not shown). Hence, Nogo-A knockout does not seem to

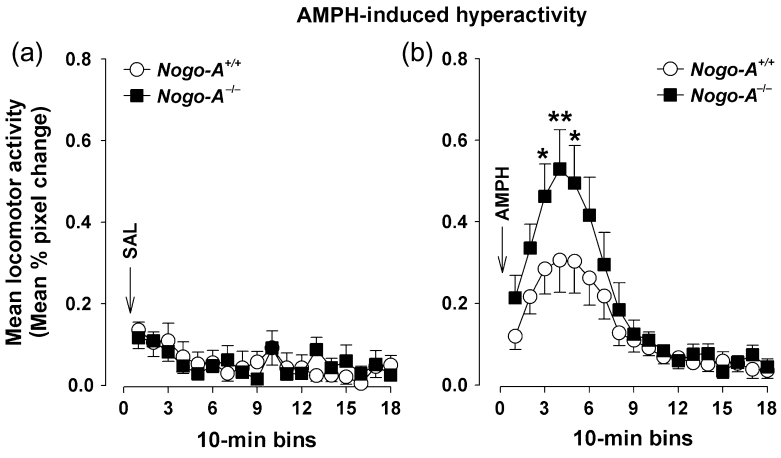

Figure 5: Enhanced sensitivity to the motor-stimulant effect of AMPH. Locomotor activity after (a) vehicle or (b) systemic AMPH administration. Both groups exhibited similar activity levels after vehicle (saline) injection (a), and the administration of AMPH led to a general increase in locomotor activity (b). However, *Nogo-A*$^{-/-}$ mice displayed significantly higher activity levels after AMPH treatment than *Nogo-A*$^{+/+}$ mice (b). Values are expressed as mean ± SEM; $n = 8$/group. SAL, saline (vehicle). *Post hoc* pairwise comparisons using Fisher's LSD with Bonferroni correction for 18 comparisons were performed on the significant genotype × 10-min bins interaction and significance is denoted by $^{*}P < 0.05$, $^{**}P < 0.01$.

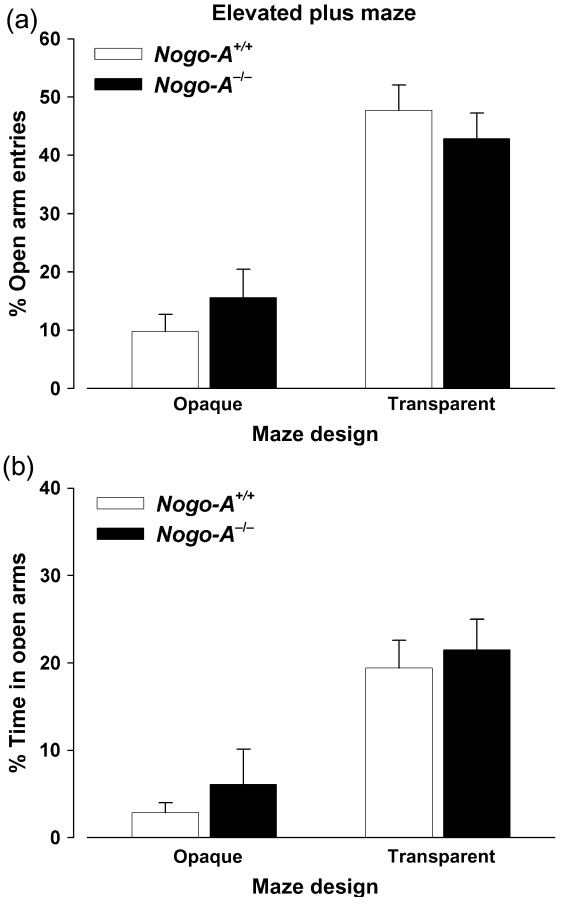

Figure 6: Normal anxiety-like behavior in the elevated plus maze in *Nogo-A*$^{-/-}$ mice. (a) Percentage of open arm entries and (b) percentage of time spent in the open arms on the elevated plus maze. Values are expressed as mean ± SEM; $n = 12$/group.

be associated with any significant changes in anxiety-related behavior.

Pavlovian associative learning is not affected in mice lacking Nogo-A

Pavlovian associative learning was assessed using the conditioned freezing paradigm (Fig. 7).

On day 1, the development of conditioned freezing was evaluated by the amount of freezing across successive presentations of the CS when it was followed by the shock US in the conditioning session. Both groups ($n = 6$/group) displayed a comparable increase in the levels of freezing in the presence of the CS across the three trials of CS–US pairings as yielded from a 2 × 3 (genotype × trials) split-plot ANOVA (trials: $F_{2,20} = 56.29$, $P < 0.001$; genotype: $F < 1$; genotype × trials: $F < 1$; Fig. 7a). On day 2, contextual freezing was evaluated (Fig. 7b) and a 2 × 8 (genotype × 1-min bins) split-plot ANOVA did not show any difference between *Nogo-A*$^{-/-}$ and *Nogo-A*$^{+/+}$ mice (genotype: $F < 1$; genotype × 1-min bins: $F < 1$).

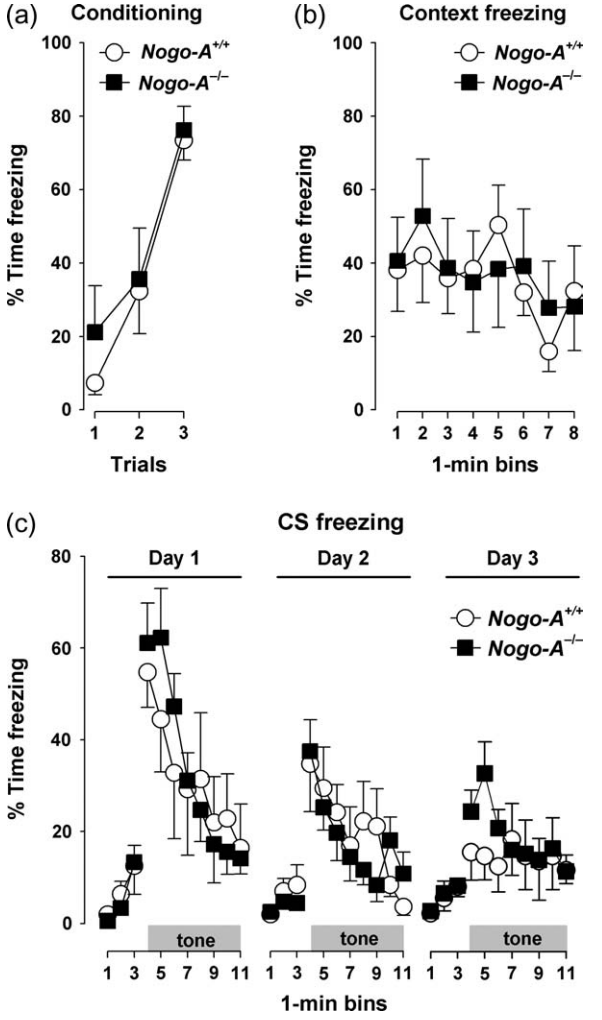

Figure 7: Unaltered conditioned freezing and extinction of fearful memories in *Nogo-A*$^{-/-}$ mice. (a) Expression of freezing behavior toward the tone CS across the three conditioning trials. (b) Percentage of time spent freezing to the context 24 h after conditioning and (c) percentage of time spent freezing to the tone CS 48, 72, and 96 h after conditioning in the conditioned freezing paradigm. Values are expressed as mean ± SEM; $n = 6$/group.

Next, conditioned freezing to the tone CS was evaluated across three successive test days (days 3–5: i.e. 48, 72 and 96 h after conditioning) as illustrated in Fig. 7c. First, the level of freezing in the 3 min before the onset of the CS was generally low and comparable between *Nogo-A*$^{-/-}$ and *Nogo-A*$^{+/+}$ mice. A 2 × 3 × 3 (genotype × days × 1-min bins) split-plot ANOVA of the pre-CS freezing levels did not yield any significant effect (all Fs < 1). Second, the expression of conditioned freezing was also comparable between groups across the 3 days of retention test. A 2 × 3 × 8 (genotype × days × 1-min bins) split-plot ANOVA of percent time freezing to the CS failed to yield any evidence of an effect of genotype or its interaction (genotype: $F < 1$; genotype × bins: $F_{7,70} = 1.82$, $P = 0.098$).

Evidence for within- as well as between-day extinction was supported by the presence of a significant main effect of bins ($F_{7,70} = 19.49$, $P < 0.001$), days ($F_{2,20} = 13.96$, $P < 0.001$) as well as their interaction ($F_{14,140} = 3.96$, $P < 0.001$). There was no evidence that the extinction learning across days was affected by the deletion of Nogo-A (genotype × days: $F < 1$).

Active avoidance learning is not affected in mice lacking Nogo-A

The two-way active avoidance paradigm involves both Pavlovian and instrumental associative learning to achieve effective avoidance learning. Acquisition of the avoidance response was evident in both groups ($n = 8$/group) as indicated by the increase in the number of avoidance responses over successive 20-trial blocks shown in Fig. 8a. This impression was supported by a main effect of 20-trial blocks ($F_{4,56} = 57.15$, $P < 0.001$) emerging from a 2 × 5 (genotype × 20-trial blocks) split-plot ANOVA of the number of avoidance responses. Consistent with the outcome of the conditioned freezing experiment, no significant group difference was detected (genotype: $F < 1$; genotype × 20-trial blocks: $F < 1$). A 2 × 5 (genotype × 20-trial blocks) split-plot ANOVA showed that the number of spontaneous shuttles during the ITI periods decreased over blocks (20-trial blocks: $F_{4,56} = 20.60$, $P < 0.001$), and this was equivalently observed in both groups (genotype: $F_{1,14} = 1.01$, $P = 0.333$; genotype × 20-trial blocks: $F_{4,56} = 2.10$, $P = 0.093$; Fig. 8b). This suggested that although *Nogo-A*$^{-/-}$ mice were exhibiting hyperactivity in home cage activity assessment (see above), this did not lead to changes in shuttle behavior here that might have confounded our evaluation of avoidance learning. Taken together, there was no indication that *Nogo-A*$^{-/-}$ mice showed any abnormality in the two paradigms of associative learning included in the present study.

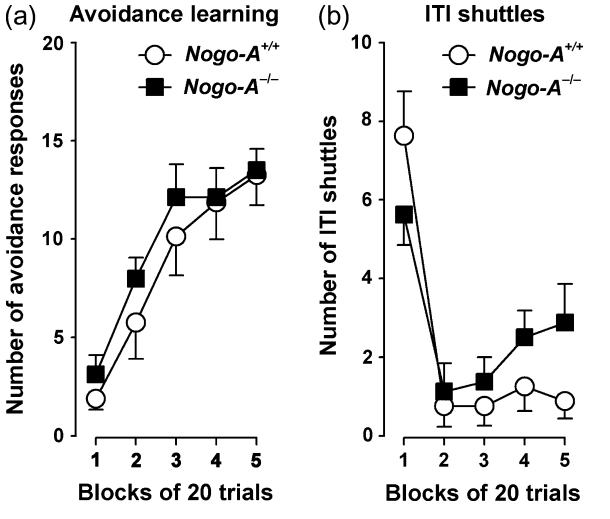

Figure 8: Unaltered conditioned avoidance learning in *Nogo-A*$^{-/-}$ mice. (a) Number of avoidance responses per block and (b) number of ITI crossings per block in the active avoidance paradigm. Values are expressed as mean ± SEM; $n = 8$/group.

Spatial learning is not affected in mice lacking Nogo-A

Next, we went on to assess spatial learning using the water maze reference memory paradigm (Fig. 9). Escape performance showed improvement during acquisition in both groups ($n = 10$–11/group), which remained comparable throughout the 5-day acquisition period (Fig. 9a). Separate 2 × 5 × 4 (genotype × days × trials) split-plot ANOVAs of escape latency and path length only yielded a significant effect of days (escape latency: $F_{4,76} = 33.03$, $P < 0.001$; path length: $F_{4,76} = 33.21$, $P < 0.001$, data not shown), but no significant effect of genotype or any interaction (all Fs < 1). No significant difference in swim speed between groups was observed (data not shown). The first probe test was conducted the day after acquisition, and search behavior distribu ted across the four quadrants during the 60-s period appeared comparable between genotypes (Fig. 9b). A 2 × 4 (genotype × quadrants) split-plot ANOVA of percentage time spent per quadrant showed a highly significant quadrants effect ($F_{3,57} = 23.68$, $P < 0.001$), but no significant effect of the factor genotype or its interaction with quadrants (genotype: $F_{1,19} = 1.40$, $P = 0.252$; genotype × quadrants: $F_{3,57} = 1.46$, $P = 0.235$). Analysis of the number of annulus crossings did also not yield an effect of genotype ($F < 1$).

Reversal learning was assessed over the next 3 days (Fig. 9c). Improvement of escape performance was evidenced by the emergence of a significant effect of days from separate 2 × 3 × 4 (genotype × days × trials) split-plot ANOVAs of escape latency and path length (escape latency: $F_{2,38} = 33.60$, $P < 0.001$; path length: $F_{2,38} = 29.18$, $P < 0.001$, data not shown). Again, no significant difference between genotypes was observed (all Fs < 1). Swim speed throughout reversal learning was also comparable between groups (data not shown). The probe test conducted the day after reversal learning yielded results highly similar to the first probe test (Fig. 9d). A 2 × 4 (genotype × quadrants) split-plot ANOVA of percentage time spent per quadrant showed a highly significant quadrants effect ($F_{3,57} = 23.08$, $P < 0.001$) but no significant effect of the factor genotype or its interaction with quadrants (Fs < 1). And again, no significant difference in the number of annulus crossings between the groups was present ($F < 1$). Hence, these data do not suggest any abnormality in spatial learning in mice lacking Nogo-A.

Discussion

In the present study, we investigated a number of basic behavioral phenotypes of mice lacking Nogo-A and provided evidence for improved motor co-ordination, the presence of spontaneous hyperactivity during the dark phase and drug-induced hyperactivity in *Nogo-A*$^{-/-}$ mice. Thus, global deletion of Nogo-A is sufficient to induce some specific behavioral changes in adulthood, while it did not lead to gross abnormalities in a wide range of behavioral domains, including various basic behavioral functions, nociception, startle reactivity, anxiety-related behavior, spatial learning and associative learning.

The role of Nogo-A in inhibiting regeneration and neurite outgrowth in the injured CNS has been well characterized

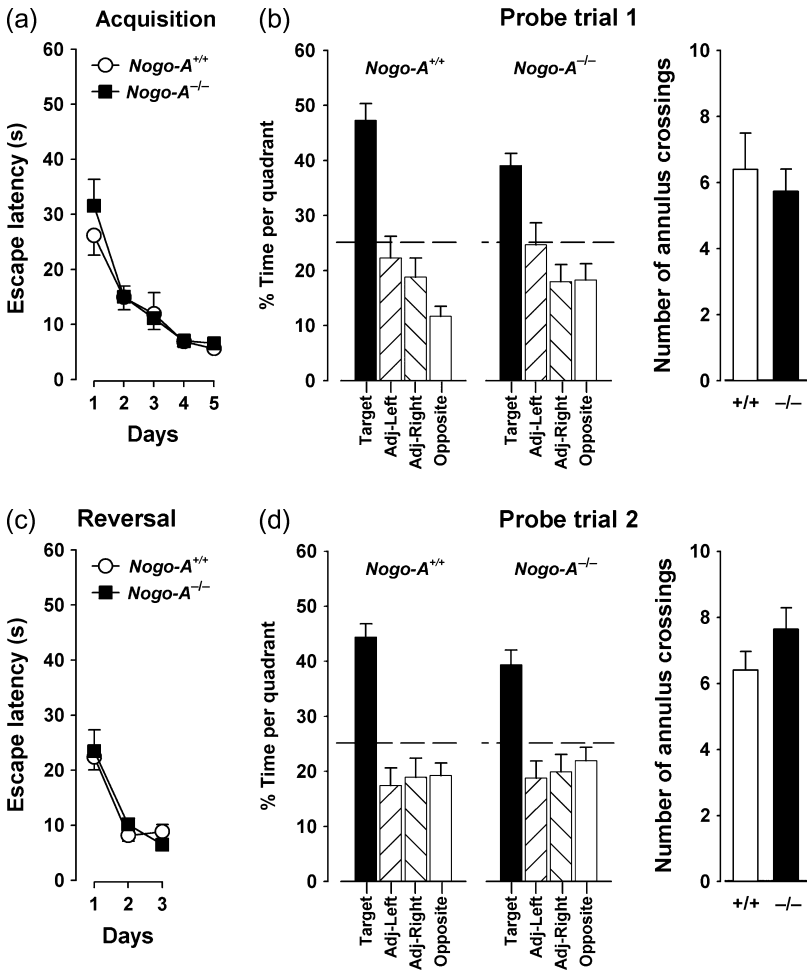

Figure 9: Unaltered spatial learning and reversal in the Morris water maze in *Nogo-A*$^{-/-}$ mice. Escape latency to reach the hidden platform during (a) acquisition and (c) reversal, respectively. Performance of search behavior, expressed as percent time spent in each quadrant and number of annulus crossings, on (b) probe trial 1 following the initial acquisition and (d) probe trial 2 following reversal learning. Values are expressed as mean ± SEM; $n = 10$ (wild-type mice), $n = 11$ (knockout mice). Target, target quadrant; Adj-Left, quadrant left adjacent to target; Adj-right, quadrant right adjacent to target; Opposite, quadrant opposite to target.

(Schwab 2004). Normally, Nogo-A (and related molecules) in the intact CNS may act as stabilizers of the highly complex CNS fiber network (Maier & Schwab 2006; McGee *et al.* 2005). In addition, the widespread distribution of Nogo-A in neurons in particular during development in the CNS as well as peripheral nervous system (Huber *et al.* 2002; Hunt *et al.* 2003; Josephson *et al.* 2001; Wang *et al.* 2002) raises serious speculation on its potential functions beyond neurite growth control. Here, our initial screening of gross behavioral expression in *Nogo-A*$^{-/-}$ mice using the SHIRPA protocol (Rogers *et al.* 1997) did not show any broad behavioral dysfunction in terms of muscle and lower motor neuron function, spinocerebellar function, sensory function and autonomic function. These findings therefore suggest that Nogo-A is not essential for such basic behavioral functions.

Neutralization of Nogo-A by specific antibody treatment has been shown to induce transient profuse sprouting of uninjured fibers (Bareyre *et al.* 2002; Buffo *et al.* 2000; L.M. Craveiro, unpublished data). Aberrant growth of primary afferent fibers in spinal cord may lead to related neuropathology such as neuropathic pain (McLachlan *et al.* 1993; Woolf & Salter 2000). We therefore evaluated this hypothesis in *Nogo-A*$^{-/-}$ mice, but did not obtain any evidence of hyperalgesia. Thus, it appears that global deletion of Nogo-A did not affect nociception. Furthermore, this suggests that pain perception could not have been a confounding factor in the interpretation of the other experiments involving potentially painful stimuli, namely, in the conditioned freezing and active avoidance experiments, in which an electric foot shock was used.

Expression of the acoustic startle reflex was also unaltered in *Nogo-A*$^{-/-}$ mice. This indicated that neither the perception of auditory stimuli nor reflexive reaction to acoustic stimulation had been altered by Nogo-A deletion. This also excluded additional confounding factors in the interpretation of the findings from the conditioned freezing and active avoidance experiments – these results were therefore not biased by potential differences in sensitivity to the auditory stimuli used.

Normal motor co-ordination and balance critically depend on the functional integrity of the brainstem and cerebellum (Lalonde & Strazielle 2007; Llinas & Welsh 1993). Interestingly, the cerebellum is one of the brain regions with high expression levels of neuronal Nogo-A: during development in Purkinje cells and throughout life in neurons of the deep cerebellar nuclei (Aloy *et al.* 2007; Huber *et al.* 2002; Hunt *et al.* 2003). *Nogo-A*$^{-/-}$ mice displayed markedly improved motor co-ordination performance compared with *Nogo-A*$^{+/+}$

animals in the rotarod test. This finding complements an earlier report showing that transgenic mice overexpressing Nogo-A in adult Purkinje cells were impaired in motor co-ordination (Aloy *et al.* 2007). The latter deficit was linked to a progressive dysfunction of Purkinje cells, especially of synapses located in deep cerebellar nuclei, suggesting that excessive Nogo-A might destabilize these synapses (Aloy *et al.* 2007). One may therefore speculate that the absence of Nogo-A might enhance synapse formation and stabilization, particularly at Purkinje cell – deep cerebellar nuclei synapses, which thereby led to the observed improvement in motor co-ordination. This concept is relevant for the results in the present study as Purkinje cells and deep cerebellar nuclei neurons express considerable levels of Nogo-A in development (Purkinje cells) or throughout life. However, the mechanisms at the physiological and network levels underlying this behavioral phenotype in *Nogo-A*$^{-/-}$ mice would certainly require further investigation and characterization.

Circadian clocks are the regulators of circadian rhythms, and they critically rely on synchronizers such as light (Cermakian & Sassone-Corsi 2000, 2002; Reppert & Weaver 2001). The underlying photoreceptive processes involve pathways going through retinal ganglion cells, targeting the suprachiasmatic nucleus, a main circadian oscillator (Cermakian & Sassone-Corsi 2000, 2002; Moore *et al.* 1995). To evaluate if Nogo-A expression in retinal ganglion cells and the hypothalamus (Funahashi *et al.* 2008; Huber *et al.* 2002; Hunt *et al.* 2003; Liu *et al.* 2002; V. Pernet, personal communication) may be essential to circadian clock-dependent processes such as the maintenance of circadian activity rhythms, we studied circadian locomotor activity under a standard 12/12-h light/dark cycle. The presence of circadian-dependent home cage locomotor activity was clearly observed in both *Nogo-A*$^{-/-}$ and *Nogo-A*$^{+/+}$ mice. Against this background, the activity level of *Nogo-A*$^{-/-}$ mice was significantly enhanced in the dark phase of the cycle relative to *Nogo-A*$^{+/+}$ mice. In the light phase, however, activity levels of the two groups were highly comparable. Given that locomotor activity is normally higher in the dark phase, whereas the light phase is characterized mainly by rest and sleep, the phase-dependent hyperactivity in *Nogo-A*$^{-/-}$ mice might be attributed to enhanced sensitivity to the stimulation by darkness. We therefore went on to study a specific form of drug-induced motor activation, and tested if the *Nogo-A*$^{-/-}$ mice would show a similar motor hypersensitivity. Increased spontaneous activity is typically associated with activation of the ascending dopaminergic projections to the striatal complex, which are in turn under the regulation of several neurotransmitters, including γ-aminobutyric acid, glutamate and acetylcholine, along with various neuropeptides (Angulo & McEwen 1994; Giros *et al.* 1996; Nestler 1994). Thus, global Nogo-A deletion might result in functional disturbances of the dopaminergic activity within the striatal circuitry in *Nogo-A*$^{-/-}$ mice, contributing to the specific hyperactivity phenotype here. Consistent with this hypothesis, *Nogo-A*$^{-/-}$ mice also displayed enhanced sensitivity to the motor-stimulating effect of the dopaminergic agonist AMPH, suggesting that the modulation of motor function by dopamine might be abnormal in *Nogo-A*$^{-/-}$ mice. However, the possible contribution of serotonergic and norepinephrinergic dysfunction (following AMPH challenge) cannot be entirely excluded (Sulzer *et al.* 2005).

The hippocampus is another brain area that contains high levels of Nogo-A even in adulthood (Huber *et al.* 2002; Meier *et al.* 2003). The hippocampal formation is a brain region with substantial neuroplastic potential and is known to play an important role in various cognitive functions as well as affective information processing (Bannerman *et al.* 2004; Davidson & Jarrard 2004; O'Keefe & Nadel 1978). In this study, we had examined the expression of anxiety-related behavior, spatial learning and two forms of fear-related associative learning known to be affected by hippocampal dysfunction or lesions (Bannerman *et al.* 2002, 2004; Bast *et al.* 2001; Kjelstrup *et al.* 2002; Maren 2001; Sanders *et al.* 2003). Anxiety-related behavior assessed using the elevated plus maze was unaltered in *Nogo-A*$^{-/-}$ mice, suggesting that loss of Nogo-A did not affect this particular form of emotional behavior. Furthermore, there was no evidence of any change in spatial water maze learning in *Nogo-A*$^{-/-}$ mice. In addition, the expression of conditioned fear acquired by associative learning mechanisms also appeared intact in *Nogo-A*$^{-/-}$ mice, suggesting that learned fear and the underlying cognitive processes involved were not grossly affected by the global absence of Nogo-A. Taken together, generally similar performances in *Nogo-A*$^{-/-}$ and *Nogo-A*$^{+/+}$ mice across the three cognitive tests that assess different forms of memory functions suggest that Nogo-A deletion does not affect mnemonic processes. Examination with additional learning paradigms, including the regulation of associative learning (e.g. by selective attentional mechanisms), perceptual learning, problem solving and choice behavior, would be necessary to further ascertain if subtle changes in cognitive functioning may be induced by the loss of Nogo-A.

The absence of gross behavioral changes in *Nogo-A*$^{-/-}$ mice shown here across a range of behavioral faculties suggests that Nogo-A is not essential to these functions, but the possibility of compensation by other functionally related proteins cannot be excluded. In fact, the expression of other neurite outgrowth inhibitors (e.g. different members of the semaphorin and ephrin families) as well as Nogo-B are substantially (up to sevenfold for Nogo-B) elevated in mice lacking Nogo-A (Dimou *et al.* 2006; Montani *et al.* 2006; Simonen *et al.* 2003). However, the functional relevance of the compensatory upregulation of any of these proteins remains speculative and would need to be directly tested, for example by examining the efficacy of antibodies designed to block specific potential compensatory proteins within the Nogo-A knockout model. Nevertheless, the data of the current study point to strong homeostatic mechanisms in the CNS, which may counteract and compensate the deletion of Nogo-A despite the pronounced fiber growth responses observed after Nogo-A inactivation. This is of direct and immediate interest to the question of potential side-effects in the ongoing clinical trials using function-blocking reagents for Nogo-A in paraplegic patients.

In conclusion, this first behavioral study of mice with constitutive genetic deletion of Nogo-A has yielded important characterization of the functional relevance of this important

membrane protein in normal brain function. While many elementary functions seem not to be contingent on the presence of Nogo-A, novel regulatory functions of this protein have been identified here with respect to motor co-ordination and circadian-dependent behavioral activation. Moreover, dopaminergic neurotransmission may play a role in the modulatory action of Nogo-A on locomotor activation. More extensive and refined assays of behavior and cognition should be encouraged to examine the possible presence of more specific and subtle behavioral changes that may be present in *Nogo-A*$^{-/-}$ mice. Following this initial study, thorough anatomical and neurochemical analyses during development as well as in the adult CNS would be highly instructive in further elucidating the mechanisms underlying the contributions of the loss of Nogo-A to the emergence of these behavioral phenotypes.

References

Aloy, E.M., Weinmann, O., Pot, C., Kasper, H., Dodd, D.A., Rulicke, T., Rossi, F. & Schwab, M.E. (2007) Synaptic destabilization by neuronal Nogo-A. *Brain Cell Biol* **35**, 137–156.

Angulo, J.A. & McEwen, B.S. (1994) Molecular aspects of neuropeptide regulation and function in the corpus striatum and nucleus accumbens. *Brain Res Rev* **19**, 1–28.

Banbury Conference on Genetic Background in Mice (1997) Mutant mice and neuroscience: recommendations concerning genetic background. *Neuron* **19**, 755–759.

Bannerman, D.M., Deacon, R.M., Offen, S., Friswell, J., Grubb, M. & Rawlins, J.N. (2002) Double dissociation of function within the hippocampus: spatial memory and hyponeophagia. *Behav Neurosci* **116**, 884–901.

Bannerman, D.M., Rawlins, J.N., McHugh, S.B., Deacon, R.M., Yee, B.K., Bast, T., Zhang, W.N., Pothuizen, H.H. & Feldon, J. (2004) Regional dissociations within the hippocampus–memory and anxiety. *Neurosci Biobehav Rev* **28**, 273–283.

Bareyre, F.M., Haudenschild, B. & Schwab, M.E. (2002) Long-lasting sprouting and gene expression changes induced by the monoclonal antibody IN-1 in the adult spinal cord. *J Neurosci* **22**, 7097–7110.

Bast, T., Zhang, W.N. & Feldon, J. (2001) Hippocampus and classical fear conditioning. *Hippocampus* **11**, 828–831.

Brosamle, C., Huber, A.B., Fiedler, M., Skerra, A. & Schwab, M.E. (2000) Regeneration of lesioned corticospinal tract fibers in the adult rat induced by a recombinant, humanized IN-1 antibody fragment. *J Neurosci* **20**, 8061–8068.

Buffo, A., Zagrebelsky, M., Huber, A.B., Skerra, A., Schwab, M.E., Strata, P. & Rossi, F. (2000) Application of neutralizing antibodies against NI-35/250 myelin-associated neurite growth inhibitory proteins to the adult rat cerebellum induces sprouting of uninjured purkinje cell axons. *J Neurosci* **20**, 2275–2286.

Caroni, P. & Schwab, M.E. (1988a) Antibody against myelin-associated inhibitor of neurite growth neutralizes nonpermissive substrate properties of CNS white matter. *Neuron* **1**, 85–96.

Caroni, P. & Schwab, M.E. (1988b) Two membrane protein fractions from rat central myelin with inhibitory properties for neurite growth and fibroblast spreading. *J Cell Biol* **106**, 1281–1288.

Cermakian, N. & Sassone-Corsi, P. (2000) Multilevel regulation of the circadian clock. *Nat Rev Mol Cell Biol* **1**, 59–67.

Cermakian, N. & Sassone-Corsi, P. (2002) Environmental stimulus perception and control of circadian clocks. *Curr Opin Neurobiol* **12**, 359–365.

Chen, M.S., Huber, A.B., van der Haar, M.E., Frank, M., Schnell, L., Spillmann, A.A., Christ, F. & Schwab, M.E. (2000) Nogo-A is a myelin-associated neurite outgrowth inhibitor and an antigen for monoclonal antibody IN-1. *Nature* **403**, 434–439.

Crawley, J.N. (2000) *What's Wrong with My Mouse? Behavioral Phenotyping of Transgenic and Knockout Mice*. Wiley-Liss, New York, NY.

Crawley, J.N., Belknap, J.K., Collins, A., Crabbe, J.C., Frankel, W., Henderson, N., Hitzemann, R.J., Maxson, S.C., Miner, L.L., Silva, A.J., Wehner, J.M., Wynshaw-Boris, A. & Paylor, R. (1997) Behavioral phenotypes of inbred mouse strains: implications and recommendations for molecular studies. *Psychopharmacology (Berl)* **132**, 107–124.

Davidson, T.L. & Jarrard, L.E. (2004) The hippocampus and inhibitory learning: a 'Gray' area? *Neurosci Biobehav Rev* **28**, 261–271.

Dimou, L., Schnell, L., Montani, L., Duncan, C., Simonen, M., Schneider, R., Liebscher, T., Gullo, M. & Schwab, M.E. (2006) Nogo-A-deficient mice reveal strain-dependent differences in axonal regeneration. *J Neurosci* **26**, 5591–5603.

Filbin, M.T. (2003) Myelin-associated inhibitors of axonal regeneration in the adult mammalian CNS. *Nat Rev Neurosci* **4**, 703–713.

Funahashi, S., Hasegawa, T., Nagano, A. & Sato, K. (2008) Differential expression patterns of messenger RNAs encoding Nogo receptors and their ligands in the rat central nervous system. *J Comp Neurol* **506**, 141–160.

Giros, B., Jaber, M., Jones, S.R., Wightman, R.M. & Caron, M.G. (1996) Hyperlocomotion and indifference to cocaine and amphetamine in mice lacking the dopamine transporter. *Nature* **379**, 606–612.

Gonzenbach, R.R. & Schwab, M.E. (2008) Disinhibition of neurite growth to repair the injured adult CNS: focusing on Nogo. *Cell Mol Life Sci* **65**, 161–176.

GrandPre, T., Nakamura, F., Vartanian, T. & Strittmatter, S.M. (2000) Identification of the Nogo inhibitor of axon regeneration as a Reticulon protein. *Nature* **403**, 439–444.

Guilding, C. & Piggins, H.D. (2007) Challenging the omnipotence of the suprachiasmatic timekeeper: are circadian oscillators present throughout the mammalian brain? *Eur J Neurosci* **25**, 3195–3216.

Hagenbuch, N., Feldon, J. & Yee, B.K. (2006) Use of the elevated plus-maze test with opaque or transparent walls in the detection of mouse strain differences and the anxiolytic effects of diazepam. *Behav Pharmacol* **17**, 31–41.

Handley, S.L. & Mithani, S. (1984) Effects of alpha-adrenoceptor agonists and antagonists in a maze-exploration model of 'fear'-motivated behaviour. *Naunyn Schmiedebergs Arch Pharmacol* **327**, 1–5.

Huber, A.B., Weinmann, O., Brosamle, C., Oertle, T. & Schwab, M.E. (2002) Patterns of Nogo mRNA and protein expression in the developing and adult rat and after CNS lesions. *J Neurosci* **22**, 3553–3567.

Hunt, D., Coffin, R.S., Prinjha, R.K., Campbell, G. & Anderson, P.N. (2003) Nogo-A expression in the intact and injured nervous system. *Mol Cell Neurosci* **24**, 1083–1102.

Josephson, A., Widenfalk, J., Widmer, H.W., Olson, L. & Spenger, C. (2001) NOGO mRNA expression in adult and fetal human and rat nervous tissue and in weight drop injury. *Exp Neurol* **169**, 319–328.

Kim, J.E., Li, S., GrandPre, T., Qiu, D. & Strittmatter, S.M. (2003) Axon regeneration in young adult mice lacking Nogo-A/B. *Neuron* **38**, 187–199.

Kjelstrup, K.G., Tuvnes, F.A., Steffenach, H.A., Murison, R., Moser, E.I. & Moser, M.B. (2002) Reduced fear expression after lesions of the ventral hippocampus. *Proc Natl Acad Sci USA* **99**, 10825–10830.

Lalonde, R. & Strazielle, C. (2007) Brain regions and genes affecting postural control. *Prog Neurobiol* **81**, 45–60.

Liebscher, T., Schnell, L., Schnell, D., Scholl, J., Schneider, R., Gullo, M., Fouad, K., Mir, A., Rausch, M., Kindler, D., Hamers, F.P. & Schwab, M.E. (2005) Nogo-A antibody improves regeneration and locomotion of spinal cord-injured rats. *Ann Neurol* **58**, 706–719.

Lister, R.G. (1987) The use of a plus-maze to measure anxiety in the mouse. *Psychopharmacology (Berl)* **92**, 180–185.

Liu, H., Ng, C.E. & Tang, B.L. (2002) Nogo-A expression in mouse central nervous system neurons. *Neurosci Lett* **328**, 257–260.

Llinas, R. & Welsh, J.P. (1993) On the cerebellum and motor learning. *Curr Opin Neurobiol* **3**, 958–965.

Maier, I.C. & Schwab, M.E. (2006) Sprouting, regeneration and circuit formation in the injured spinal cord: factors and activity. *Philos Trans R Soc Lond B Biol Sci* **361**, 1611–1634.

Maren, S. (2001) Neurobiology of Pavlovian fear conditioning. *Annu Rev Neurosci* **24**, 897–931.

McGee, A.W., Yang, Y., Fischer, Q.S., Daw, N.W. & Strittmatter, S.M. (2005) Experience-driven plasticity of visual cortex limited by myelin and Nogo receptor. *Science* **309**, 2222–2226.
McLachlan, E.M., Janig, W., Devor, M. & Michaelis, M. (1993) Peripheral nerve injury triggers noradrenergic sprouting within dorsal root ganglia. *Nature* **363**, 543–546.
Meier, S., Brauer, A.U., Heimrich, B., Schwab, M.E., Nitsch, R. & Savaskan, N.E. (2003) Molecular analysis of Nogo expression in the hippocampus during development and following lesion and seizure. *FASEB J* **17**, 1153–1155.
Merkler, D., Metz, G.A., Raineteau, O., Dietz, V., Schwab, M.E. & Fouad, K. (2001) Locomotor recovery in spinal cord-injured rats treated with an antibody neutralizing the myelin-associated neurite growth inhibitor Nogo-A. *J Neurosci* **21**, 3665–3673.
Meyer, U., Feldon, J., Schedlowski, M. & Yee, B.K. (2005) Towards an immuno-precipitated neurodevelopmental animal model of schizophrenia. *Neurosci Biobehav Rev* **29**, 913–947.
Meyer, U., Murray, P.J., Urwyler, A., Yee, B.K., Schedlowski, M. & Feldon, J. (2008) Adult behavioral and pharmacological dysfunctions following disruption of the fetal brain balance between pro-inflammatory and IL-10-mediated anti-inflammatory signaling. *Mol Psychiatry* **13**, 208–221.
Montani, L., Petrinovic, M., Dimou, L. & Schwab, M.E. (2006) Knock-out for Nogo: molecular mechanisms of regeneration in the CNS, a genomic/proteomic approach. *Abstr Soc Neurosci* **32**, 618.
Moore, R.Y., Speh, J.C. & Card, J.P. (1995) The retinohypothalamic tract originates from a distinct subset of retinal ganglion cells. *J Comp Neurol* **352**, 351–366.
Nestler, E.J. (1994) Hard target: understanding dopaminergic neurotransmission. *Cell* **79**, 923–926.
O'Keefe, J. & Nadel, L. (1978) *The Hippocampus as a Cognitive Map*. Oxford University Press, Oxford.
Pellow, S., Chopin, P., File, S.E. & Briley, M. (1985) Validation of open: closed arm entries in an elevated plus-maze as a measure of anxiety in the rat. *J Neurosci Methods* **14**, 149–167.
Pietropaolo, S., Feldon, J. & Yee, B.K. (2008a) Nonphysical contact between cagemates alleviates the social isolation syndrome in C57BL/6 male mice. *Behav Neurosci* **122**, 505–515.
Pietropaolo, S., Sun, Y., Li, R., Brana, C., Feldon, J. & Yee, B.K. (2008b) The impact of voluntary exercise on mental health in rodents: a neuroplasticity perspective. *Behav Brain Res* **192**, 42–60.
Prinjha, R., Moore, S.E., Vinson, M., Blake, S., Morrow, R., Christie, G., Michalovich, D., Simmons, D.L. & Walsh, F.S. (2000) Inhibitor of neurite outgrowth in humans. *Nature* **403**, 383–384.
Reppert, S.M. & Weaver, D.R. (2001) Molecular analysis of mammalian circadian rhythms. *Annu Rev Physiol* **63**, 647–676.
Richmond, M.A., Murphy, C.A., Pouzet, B., Schmid, P., Rawlins, J.N. & Feldon, J. (1998) A computer controlled analysis of freezing behaviour. *J Neurosci Methods* **86**, 91–99.
Rogers, D.C., Fisher, E.M., Brown, S.D., Peters, J., Hunter, A.J. & Martin, J.E. (1997) Behavioral and functional analysis of mouse phenotype: SHIRPA, a proposed protocol for comprehensive phenotype assessment. *Mamm Genome* **8**, 711–713.
Russig, H., Durrer, A., Yee, B.K., Murphy, C.A. & Feldon, J. (2003) The acquisition, retention and reversal of spatial learning in the Morris water maze task following withdrawal from an escalating dosage schedule of amphetamine in Wistar rats. *Neuroscience* **119**, 167–179.
Sanders, M.J., Wiltgen, B.J. & Fanselow, M.S. (2003) The place of the hippocampus in fear conditioning. *Eur J Pharmacol* **463**, 217–223.
Schnell, L. & Schwab, M.E. (1990) Axonal regeneration in the rat spinal cord produced by an antibody against myelin-associated neurite growth inhibitors. *Nature* **343**, 269–272.
Schwab, M.E. (2002) Increasing plasticity and functional recovery of the lesioned spinal cord. *Prog Brain Res* **137**, 351–359.
Schwab, M.E. (2004) Nogo and axon regeneration. *Curr Opin Neurobiol* **14**, 118–124.
Simonen, M., Pedersen, V., Weinmann, O., Schnell, L., Buss, A., Ledermann, B., Christ, F., Sansig, G., van der Putten, H. & Schwab, M.E. (2003) Systemic deletion of the myelin-associated outgrowth inhibitor Nogo-A improves regenerative and plastic responses after spinal cord injury. *Neuron* **38**, 201–211.
Spillmann, A.A., Bandtlow, C.E., Lottspeich, F., Keller, F. & Schwab, M.E. (1998) Identification and characterization of a bovine neurite growth inhibitor (bNI-220). *J Biol Chem* **273**, 19283–19293.
Sulzer, D., Sonders, M.S., Poulsen, N.W. & Galli, A. (2005) Mechanisms of neurotransmitter release by amphetamines: a review. *Prog Neurobiol* **75**, 406–433.
Wang, X., Chun, S.J., Treloar, H., Vartanian, T., Greer, C.A. & Strittmatter, S.M. (2002) Localization of Nogo-A and Nogo-66 receptor proteins at sites of axon-myelin and synaptic contact. *J Neurosci* **22**, 5505–5515.
Woolf, C.J. & Salter, M.W. (2000) Neuronal plasticity: increasing the gain in pain. *Science* **288**, 1765–1769.

Acknowledgments

The present study was supported by grants of the Swiss National Science Foundation (31-63633.00), the National Center for Competence in Research 'Neural Plasticity & Repair' of the Swiss National Science Foundation, the Spinal Cord Consortium of the Christopher and Dana Reeve Foundation (Springfield, NJ, USA), and the EU Network of Excellence NeuroNE. We are extremely grateful to the National Center for Competence in Research 'Neural Plasticity & Repair' for facilitating the collaboration between our research groups. Special thanks also to Miriam Gullo and Peter Schmid for excellent technical assistance, to Franziska Christ for animal breeding and to the Animal Services Department in Schwerzenbach (ETH Zurich) for animal care.